Organometallic Bond Dissociation Energies: Laser Pyrolysis of $Fe(CO)_5$, $Cr(CO)_6$, $Mo(CO)_6$, and $W(CO)_6$

Karan E. Lewis, David M. Golden, and Gregory P. Smith*

Contribution from the Department of Chemical Kinetics, SRI International, Menlo Park, California 94025. *Received September 9, 1983*

Abstract: A pulsed laser pyrolysis technique has been used to study the gas-phase thermal decomposition of iron pentacarbonyl, chromium hexacarbonyl, molybdenum hexacarbonyl, and tungsten hexacarbonyl. Arrhenius parameters were determined by comparative rate measurements, relative to dicyclopentadiene decomposition. The respective first bond dissociation energies are 41, 37, 40, and 46 kcal/mol (±2), with log A measured to be 15.5–16.0. For chromium hexacarbonyl decomposition only, the rate-determining step is a subsequent bond scission, with a 40 kcal/mol activation energy. Bond dissociation energies for other ligands in monosubstituted carbonyls have been derived from thermodynamic data and the current results.

Rapid advances in the fields of homogeneous and heterogeneous catalysis have underlined the importance of organometallic compounds and their bonding in catalytic and synthetic processes. A quantitative understanding of the relationships between the structure, bonding, and reactivity of these compounds would enable us to better understand currently useful processes and perhaps suggest modifications and improvements. This requires a knowledge of kinetic parameters and bond dissociation energies (BDEs) for the individual species involved. Such basic thermodynamic information is vital in determining the intermediates involved in various catalytic mechanisms. To understand known reactions and predict new ones, one must know the strengths of the bonds being broken and made. It may also prove possible to relate these values to the thermochemistry of heterogeneous processes. In addition, a better understanding of organometallic bond dissociation energies can suggest whether proposed new catalytic systems may work well.

We consider here the broad class of carbonyl compounds, given the vast array of important processes involving CO. One relevant example of the importance of BDEs is the hydroformylation reaction which uses a carbonyl catalyst to convert an alkene into an aldehyde. According to typical mechanisms,[1] a complete thermodynamic and kinetic characterization of this system requires knowledge of the metal carbonyl bond strengths to CO, as well as to alkenes, alkyl groups, acyl groups, and hydrogen.

Unlike the hydrocarbons, few organometallic BDE's have been determined. A few recent solution[2] and ionic[3] values exist, and some relative values can be derived from the limited available thermodynamic data.[4] One major difficulty often preventing successful studies of organometallic bond energies is the general surface reactivity of these compounds, which decompose catalytically in conventional experiments. We have developed a pulsed laser technique[5] which provides rapid, indirect thermal heating and cooling to study homogeneous gas-phase decompositions. Since cell walls remain cool, heterogeneous processes are avoided. As part of a program to measure neutral organometallic gas-phase decomposition kinetics and BDE's, we report here laser pyrolysis measurements and bond energies for the bond scission kinetics of four mononuclear metal carbonyls, $Fe(CO)_5$, $Cr(CO)_6$, $Mo(CO)_6$, and $W(CO)_6$.

Such carbonyls represent a particularly important class of transition-metal compounds for which bond energies need to be determined. A major fraction of the extensive organometallic and catalysis literature concerns carbonyl compounds and mechanisms. Basic bond energy data are critical to understanding this work and to the consideration of new systems in the future. In addition, the catalytic relevance of carbonyl compounds, dissociation products, and intermediates noted earlier also extends to newer cluster catalysis[6] work and to other useful, important processes involving ligand dissociation and substitution mechanisms.[7] Gas-phase studies can help clarify solvent effects in prior work. The large number of tractable carbonyl compounds provides a good comparative series to examine effects and trends in transition-metal complex bonding. Other bond energies can be derived from these measurements and existing or future thermochemical data. CO is a prototypical back-bonding ligand, involving the metal d-orbitals. Thus, bond energy measurements for CO should provide theoreticians a good bench mark as they attempt reliable calculations relevant to understanding organometallic bonding and mechanisms.

Other relevant investigations on metal carbonyls include theoretical calculations[8-10] and some experimental measurements on carbonyl bond scission fragments.[11] Considerable recent work concerns photolysis processes,[6,12] often multiphoton, for these carbonyls in the gas phase. This pyrolysis work is needed for comparison and can provide parameters necessary to interpret the photoprocess.

The method of pulsed-laser pyrolysis, a technique which we have recently used to study unimolecular reactions,[5] will be described in detail in the Experimental Section. In essence, a pulsed infrared CO_2 laser is used to heat an absorbing gas (SF_6), which then collisionally transfers its energy to the reactive substrate and bath gas (N_2). Surfaces remain cool. Fractional decomposition is measured later by using a mass spectrometric detection system. A kinetically well-characterized internal standard is used to define the reaction temperature. Use of a heated flow system makes the technique suitable for low vapor pressure substrates. Laser pyrolysis offers several advantages over other techniques. Gas-phase measurements avoid possible problems created by solvent or matrix effects on the molecules. Laser heating provides a wide temperature range and short, well-controlled, reaction times. (Most

(1) Halpern, J. *Annu. Rev. Phys. Chem.* **1965**, *16*, 103. Toman, G. A. *Chem. Soc. Rev.* **1972**, *1*, 337.
(2) Halpern, J. *Acc. Chem. Res.* **1982**, *15*, 238.
(3) Armentrout, P. B.; Beauchamp, J. L. *J. Am. Chem. Soc.* **1981**, *103*, 782 and references therein. Foster, M. S. Beauchamp, J. L. **1975**, *97*, 4808.
(4) Connor, J. A. *Curr. Top. Chem.* **1977**, *71*, 71.
(5) McMillen, D. M.; Lewis, K. E.; Smith, G. P.; Golden, D. M. *J. Phys. Chem.* **1982**, *86*, 709.
(6) Maugh, T. H. *Science (Washington, D.C.)* **1983**, *220*, 592.
(7) Wender, I.; Pino, P. "Organic Synthesis via Metal Carbonyls"; Wiley: New York, 1968; Vol. 1.
(8) Burdett, J. K. *J. Chem. Soc., Faraday Trans. 2* **1974**, *70*, 1599.
(9) Hay, P. J. *J. Am. Chem. Soc.* **1978**, *100*, 2411.
(10) Sherwood, D. E.; Hall, M. B. *Inorg. Chem.* **1983**, *22*, 93; **1980**, *19*, 1805 and references therein.
(11) Perutz, R. N.; Turner, J. J. *J. Am. Chem. Soc.* **1975**, *97*, 4791. Davies, B.; McNeish, A.; Poliakoff, M.; Turner, J. J. *Ibid.* **1977**, *99*, 7573. Davies, B.; McNesh, A.; Poliakoff, M.; Tranquille, M.; Turner, J. J. *Chem. Phys. Lett.* **1978**, *52*, 477.
(12) Karny, Z.; Naamen, R.; Zare, R. N. *Chem. Phys. Lett.* **1978**, *59*, 33. Garity, D. P.; Rathberg, L. J.; Vaida, V. *J. Phys. Chem.* **1983**, *87*, 2222. Breckenridge, W. H.; Sinai, N. *Ibid.* **1981**, *85*, 3557.
(13) Whetten, R. L.; Fu, K. F.; Grant, E. R. *J. Chem. Phys.* **1982**, *77*, 3769.
(14) Nathanson, G.; Gitlin, B.; Rosan, A. M.; Yardley, J. T. *J. Chem. Phys.* **1981**, *74*, 361. Tumas, W.; Gitlin, B.; Rosan, A. M.; Yardley, J. T. *J. Am. Chem. Soc.* **1982**, *104*, 55.
(15) Ouderkirk, A. J.; Wermer, P.; Schultz, N. L.; Weitz, E. *J. Am. Chem. Soc.* **1983**, *105*, 3354. Ouderkirk, A. J.; Weitz, E. *J. Chem. Phys.* **1983**, *79*, 1089.
(16) Fletcher, T. R.; Rosenfeld, R. N. *J. Am. Chem. Soc.* **1983**, *105*, 6358.

0002-7863/84/1506-3905$01.50/0

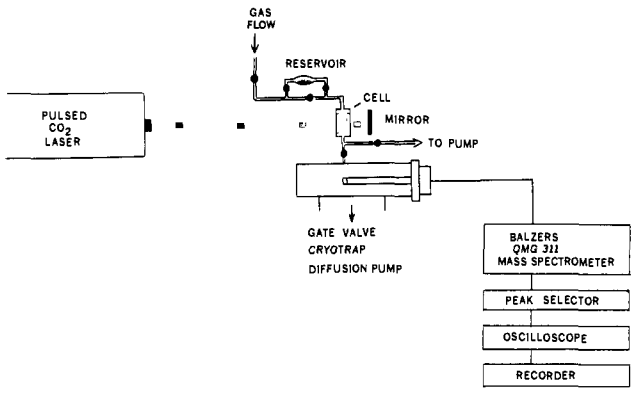

Figure 1. Schematic diagram of the pulsed laser pyrolysis apparatus.

reactions are ended by expansion cooling after 10 μs.) Using a pulsed laser results in rapid heating and cooling, which helps to minimize secondary reactions. Most importantly, under these conditions, we have an effectively wall-less reactor, and surface catalysis is avoided.

The technique, apparatus, and data analysis are discussed in the Experimental Section. The Results section presents the relative decomposition rate data and other observations, a detailed discussion of the interpretation of the $Cr(CO)_6$ results, and consideration of pressure fall-off effects. The Discussion section examines the results in terms of the work of others, derives some values for other ligands (mostly amines), and considers any trends, comparisons, or implications from these results.

Experimental Section

Laser pyrolysis was first developed by Shaub and Bauer[17] as a CW technique and later modified, tested, and applied by our group[5,18] and others,[19] using a pulsed laser. Since the physics of the method are fully described in detail elsewhere,[5,18] including computational, spectroscopic, and chemical diagnostics and confirmations, only a brief account will be presented here. A slow flow of a few torr of SF_6 in 100-torr N_2 bath gas, with small amounts of the carbonyl and a chemical temperature standard, is passed through a thin cylindrical cell. A portion of the cell is irradiated by a uniform pulsed CO_2 laser beam, and the SF_6 absorbs a fraction of the energy. This vibrational energy is collisionally transferred to the bath gas, reaching a true, equilibrated temperature in a few microseconds. The gas in the irradiated volume, including the reactants, is now at high temperature and pressure with respect to the surrounding gas. Expansion accompanied by cooling now occurs, accomplished by a rarefaction wave propagating inward through the heated region at the local speed of sound. For an initial 850 K temperature, this cooling is roughly 200 K and effectively quenches further rate-determining (high E_a) unimolecular reactions. For our 1.8-cm diameter laser beam, cooling requires 16 μs, and the average reaction time, t_r, is ~8 μs. Since the cooling is accompanied by an outward propagating compression wave, an off-axis geometry is required to prevent reheating of the gas by reflected shockwaves. Further slow cooling (~1 K/μs) to 300 K occurs by thermal conductivity and diffusion prior to the next laser pulse.

Measurement of reaction yields is accomplished by mass spectrometric monitoring of reactant concentrations in the flowing gas mixture downstream from the reaction cell. The quantitative carbonyl reaction kinetics were determined by a comparative rate technique with a compound whose kinetic parameters are known and which produces stable products. The temperature standard used here was the revese Diels–Alder decomposition of dicyclopentadiene ($\log k = 13.0 - (34.1\ (\pm 0.5))/(2.3RT)$).[20] An added advantage of this method is that minor temperature inhomogeneities have little effect on the results.

The experimental apparatus is illustrated schematically in Figure 1. A flowing as mixture of carbonyl, temperature standard, SF_6, and N_2 at <0.1, 0.1, 3.0, and 97.0 torr, respectively, is directed through a 3.8-cm diameter, 1.25-cm thick cell. Flow times, that is, cell residence times, of ~1–3 min were measured by a pressure transducer from a calibrated volume behind the initial flow control needle valve. The exit needle valve controls the cell pressure which is monitored by a second transducer. For the low vapor pressure $Mo(CO)_6$ and $W(CO)_6$, a heated reservoir with capillary inlet and outlet in the flow line prior to the cell was used for the addition of carbonyl to the sample. Decay of the mass spectrometer signal when the reservoir was closed confirms the same residence time as that measured for the gas mixture flow. The flow line is heated to ~320 K, above the reservoir temperature, to avoid condensation problems.

The cell is irradiated at 0.25 Hz by the P(20), 10.6-μm output of a Lumonics K103 CO_2 laser (duration 1 μs, fluence 1 J/cm^2). The cell has KCl windows to transmit the radiation, a 1.8-cm-diameter laser-beam aperture to define an even heating volume, and a rear-reflecting mirror to ensure axial temperature homogeneity in view of the ~20% laser absorption on a single pass. Reaction temperature is controlled by attenuating the laser and adjusting the SF_6 content of the gas mixture. The chosen flow times and irradiation frequency ensure averaging over ~20 laser shots and complete gas mixing between shots.

The flowing gas downstream of the reaction cell was monitored by a Balzers QMG 311 mass spectrometer, the amplified output being recorded on a strip chart recorder. Dicyclopentadiene and $Cr(CO)_6$ were monitored at their parent peaks (m/e 132 and 220), while $Fe(CO)_5$, $Mo(CO)_6$, and $W(CO)_6$ were monitored at m/e 80 ($FeCO^+$), 180 ($Mo(CO)_3^+$), and 184 (W^+), respectively. It was determined that all peaks in the carbonyl mass spectra faithfully track the parent peak intensity upon irradiation.

Since the lack of volatile carbonyl pyrolysis products dictates analysis by monitoring disappearance of reaction products, the range of decomposition yields in the flow which can be accurately measured is 5–90%. Products of the temperature standard also cannot be quantitatively measured at low yields due to large mass spectra interferences from the undecomposed molecules. Thus, the temperature standard and unknown should have similar rates to permit accurate measurements over a significant temperature range. This also minimizes the effects of any systematic errors. The accuracy of this technique for compounds of differing activation energies is discussed in ref 5. Molecular elimination reactions are favored as standards since secondary radical chain reactions are prevented. For these experiments, $Cr(CO)_6$ decomposition was measured relative to that of dicyclopentadiene. The other carbonyls were measured relative to the chromium compound.

The reaction yield kt_r is given by[5]

$$kt_r = -\ln\,[1 - ((A_0/A) - 1)(V_T/V_R)(t_L/t_F)] \qquad (1)$$

where A_0 and A are the initial and irradiated steady-state concentrations of substrate determined mass spectrometrically, V_T/V_R is the ratio of cell to irradiated volume, and t_L/t_F is the ratio of the time between laser shots and the measured flow lifetime. Given the Arrhenius form for each rate, $k = A\,e^{-E/RT}$, and plotting $\log k_1t_r$ vs. $\log k_2t_r$, we get a line described by[5]

$$\log k_1t_r = \log A_1 + (1 - E_1/E_2)\log t_r - (E_1/E_2)\log A_2 + (E_1/E_2)\log k_2t_r \qquad (2)$$

The slope of this comparative rate plot is E_1/E_2, and therefore, knowledge of E_2 furnishes the unknown activation energy E_1. From the intercept and known values of t_r and A_2, the value of A_1 can be also determined.

Results and Analysis

Figure 2 is a logarithmic relative rate plot for the decomposition of $Cr(CO)_6$ under laser pyrolysis conditions vs. that of dicyclopentadiene to two cyclopentadiene molecules. Least-squares analysis gives a slope of 1.34 ± 0.05 and an intercept (base e) of 3.17 ± 0.17, which coupled with the literature values for dicyclopentadiene gives $\log k\ (Cr(CO)_6) = 17.18 - 45.5/(2.3RT)$. E_a is in kcal/mol. A few experiments were performed with $Cr(CO)_6$ in the reservoir, which could be bypassed, to see if the dicyclopentadiene decomposition rate for a given fluence, gas mixture, and flow rate varied when $Cr(CO)_6$ or its pyrolysis products were absent or present. No difference was observed, indicating dicyclopentadiene decomposition is not catalyzed by $Cr(CO)_6$ or any pyrolysis products in the gas phase. (Thus, unlike in solution, no cyclopentadiene ligand substitution is observed.)

Simultaneous rate measurements were performed on pairs of carbonyls, with the molybdenum, tungsten, and iron compound decompositions measured relative to that of chromium. The respective results are presented in Figures 3–5. Again, no catalytic

(17) Shaub, W. M.; Bauer, S. H. *Int. J. Chem. Kinet.* **1975**, *7*, 509. Shaub, W. M. Ph.D. Thesis, Cornell University, Ithaca, NY 1975.

(18) Fairchild, P. W.; Smith, G. P.; Crosley, D. R.; 19th Symposium (International) on Combustion, 1982, pp 107–115. *J. Chem. Phys.*, in press.

(19) Steel, C.; Starov, V.; Leo, R.; John, P.; Harrison, R. G. *Chem. Phys. Lett.* **1979**, *62*, 121. Dau, H. L.; Specht, E.; Berman, M. R.; Moore, C. B. *J. Chem. Phys.* **1982**, *77*, 4494.

(20) Herndon, W. C.; Grayson, C. R.; Manion, J. M. *J. Org. Chem.* **1967**, *32*, 526.

Table I. Summary of Laser Pyrolysis Results

compd	T, K	E_a, kcal/mol	log A	k/k_∞	log A_∞	E_a^∞, kcal/mol	$\Delta H°_{298}$, kcal/mol
$Cr(CO)_6$	740–820	45.5 ± 1.8	17.2				
		(35.3)[a]	(15.4)	(0.75)	(15.5)	(35.3)	(36.8)
$Mo(CO)_6$	670–760	38.9 ± 2.4	15.4 ± 0.8	0.80–0.79	15.6	39.0	(40.5)
$W(CO)_6$	745–810	44.3 ± 2.8	15.5 ± 0.7	0.90–0.86	15.6	44.5	(46.0)
$Fe(CO)_5$	670–780	39.6 ± 2.3	15.7 ± 0.8	0.88–0.80	15.8	40.0	(41.5)

[a] See text.

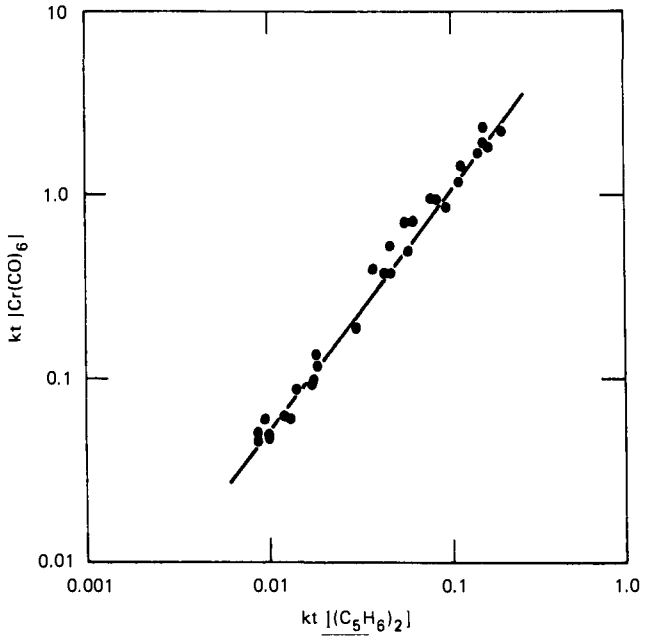

Figure 2. Logarithmic comparative rate plot for chromium hexacarbonyl vs. dicyclopentadiene decomposition. (Line is least-squares fit.)

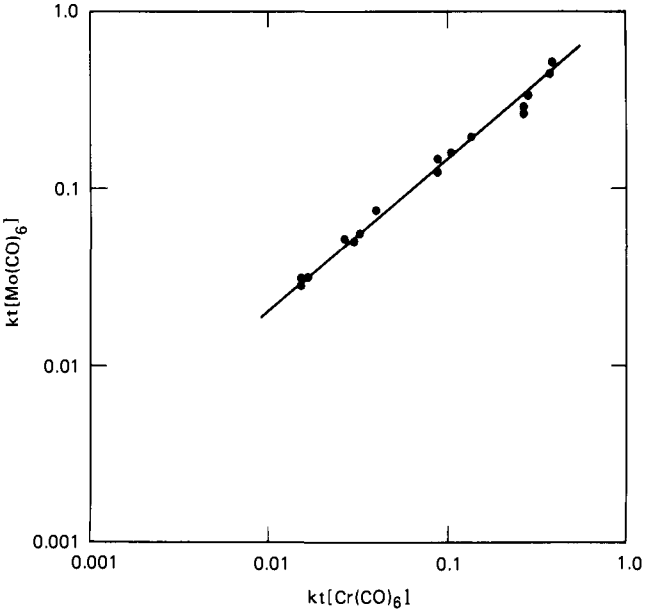

Figure 3. Logarithmic comparative rate plot for molybdenum hexacarbonyl vs. chromium hexacarbonyl decomposition. (Least-squares line slope is 0.856 ± 0.028.)

effects upon the decomposition were observed when rate measurements were done independently or coincidentally on pairs of carbonyls under identical experimental conditions. The Arrhenius parameters calculated from the data in Figures 2–5 are summarized in Table I, with other entries to be discussed later. Note the large log A value for $Cr(CO)_6$. The experimental temperature ranges are derived from the absolute yields of the temperature

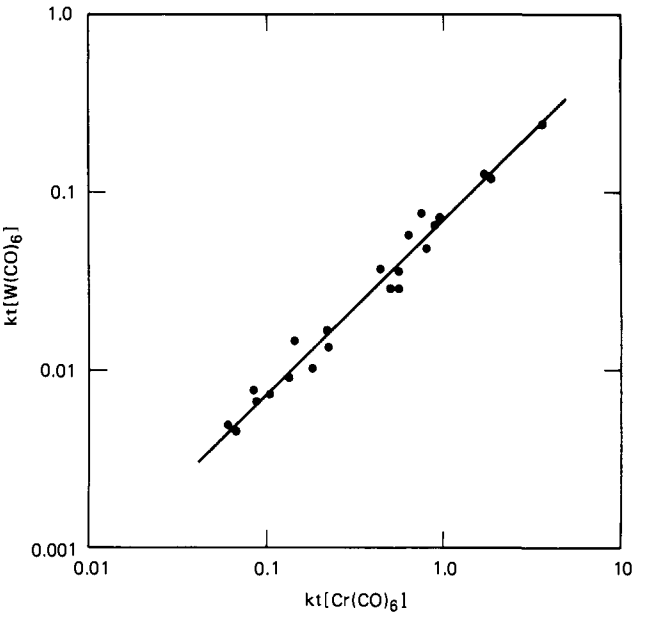

Figure 4. Logarithmic comparative rate plot for tungsten hexacarbonyl vs. chromium hexacarbonyl decomposition. (Least-squares line slope is 0.974 ± 0.038.)

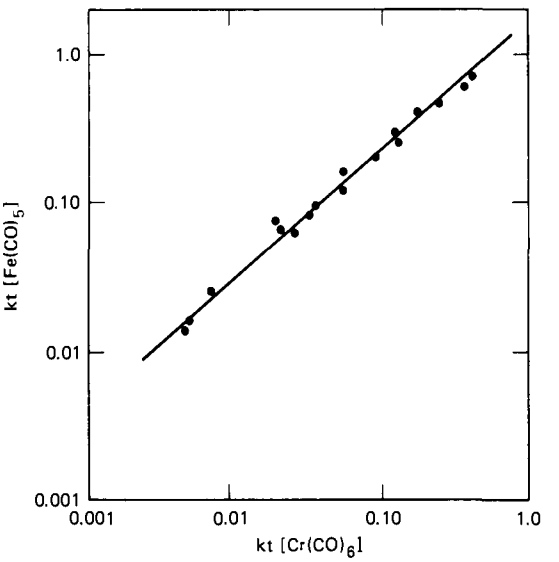

Figure 5. Logarithmic comparative rate plot for iron pentacarbonyl vs. chromium hexacarbonyl decomposition. (Least-squares line slope is 0.870 ± 0.030.)

standard decomposition for the respective experiments assuming t_r = 10 μs. The quoted errors are 1σ, propagated by sum of squares.

To examine the consistency of the results, $Fe(CO)_5$ decomposition was also measured relative to $Mo(CO)_6$ and gave a log–log slope of 1.01 ± 0.09. This agrees with the 1.02 value predicted by the individual runs relative to $Cr(CO)_6$. The magnitude of the relative rates (A factors) is also consistent with the earlier results.

Table II. Comparative Rate Measurements for $Cr(CO)_6$ vs. *t*-BuI

		kt[*t*-BuI]		
T, K	$kt[Cr(CO)_6]$	no Cr	with Cr	E_a (log A = 17.18)
829	1.3	0.052		46.0
817	1.1	0.037		45.6
797	1.1	0.021	0.43	44.5
800	0.69	0.023	0.24	44.4
779	0.53	0.012		44.6
772	0.23	0.0096	0.082	45.5
769	0.26	0.0088	0.105	45.2
761	0.32	0.0068		44.4
				45.2 ± 0.2 av

To test the procedure of determining the other carbonyl rates through the calibrated value for chromium, a few measurements were also made for $Fe(CO)_5$, vs. dicyclopentadiene. Two points were taken, at 772 and 800 K, according to the measured dicyclopentadiene yields. Assuming a $Fe(CO)_5$ log A value of 15.7 as before, the measured $Fe(CO)_5$ rates give E_a = 39.6 and 40.0 kcal/mol. This value, and thus the relative rates, matches the 39.6-kcal value derived from the data relative to $Cr(CO)_6$ of Figures 2 and 3.

The reported log A = 13.0 for dicyclopentadiene seems somewhat low (kT/h alone is $10^{13.2}$ at 750 K). Also, the dicyclopentadiene appeared to stick on the heated sampling line, at times giving residence times (determined by using the mass spectrometer) which were 60% longer than other species based on the transducer value. (The analysis in figure 2 used this longer measured τ_f for dicyclopentadiene only.) The chief effect of both these factors is one of ~0.3 on log A values. To examine these potential complications and to confirm the use of the dicyclopentadiene standard, alternate temperature standards were examined. Metal carbonyls and the fragments resulting from their decomposition, unfortunately, catalyzed the decomposition of several of the temperature standards that were initially tried. Large increases in decomposition rate were observed for paraldehyde (the cyclic trimer of acetaldehyde) and *tert*-butyl iodide when $Cr(CO)_6$ was present. As an example, comparative rate measurements for $Cr(CO)_6$ relative to *tert*-butyl iodide are presented in Table II.

Rate parameters for *t*-BuI are reported[21] to be

$$t\text{-BuI} \rightarrow C_4H_8 + HI$$

$$\log k = 13.7 - 38.1/\theta$$

The special reservoir for the metal carbonyl was set up so that the carrier flow could be diverted around it as well as through it, and the decomposition of the *t*-BuI could be measured independently of the carbonyl, at the same laser fluence and flow rate. Temperatures were determined from the fractional decomposition of the uncatalyzed *t*-BuI. The large discrepancies in the *t*-BuI rate with and without $Cr(CO)_6$ present are clearly seen. There is some additional scatter in these data due to shot-to-shot laser fluctuations (which cancel out when simultaneous measurements are made). An activation energy for the carbonyl can be calculated for each run by using the temperature calculated from the uncatalyzed *t*-BuI rate and the $Cr(CO)_6$ A-factor of Table I. The resulting $Cr(CO)_6$ activation energy closely matches that derived from the dicyclopentadiene comparative rate experiments, indicating two compatible sets of standardized data. Conversely, when E_a = 45.5 kcal is used, the data of Table II yield log A = 17.25.

The laser pyrolysis decomposition products of $Fe(CO)_5$ were also observed to catalyze the decomposition of *tert*-butyl iodide and paraldehyde. Isopropyl iodide decomposition, however, with a 7 kcal higher activation energy,[21] was not catalyzed under laser pyrolysis conditions of partial $Cr(CO)_6$ decomposition. Thus, the dehydrohalogenation catalysis apparently proceeds by only a modest lowering of energy barriers.

The final products in the laser pyrolysis of the iron, molybdenum, and tungsten carbonyls result in a layer of dark, small particles on the cell, presumably mostly metal. The iron particles responded to a magnet, and analysis revealed <2% carbon content. Since the CO ligands were the only carbon or oxygen source in the cell, the particulates likely contain little oxygen also. Following each pulse of $Fe(CO)_5$ laser pyrolysis, a fine mist of small particles can be seen in the gas, either by visualization or by He–Ne laser light scattering within 20 μs of the CO_2 laser pulse. In addition, the presence of iron atoms has been determined by laser-induced fluorescence. These results suggest that the iron (and presumably molybdenum and tungsten) carbonyl loses its remaining CO ligands rapidly after the initial decomposition step. This is in accord with a higher temperature shock-tube study of $Fe(CO)_5$ decomposition, which was used to study iron atom nucleation[22] Laser pyrolysis of carbonyls should prove useful for such studies, although fragment species other than metal atoms may participate in the nucleation process. The measured carbonyl decomposition rates were independent of the buildup of metal particulates on cell walls and windows and were independent of the concentration of carbonyl, hence aerosol particles, used. This indicates surface and self-catalysis, a severe problem for conventional pyrolysis studies, is not a difficulty here.

The $Cr(CO)_6$ showed no signs of such a nucleation process. Even when irradiated for more than 1 h at laser fluences sufficient to decompose all $Cr(CO)_6$, no traces of particles, or any product, were observed on the cell walls or in the mass spectrometer. The cause of this different behavior and the fate of the decomposed $Cr(CO)_6$ product remain unclear.

Having determined the kinetic parameters for the metal carbonyl decompositions, the next step is to determine the basic reaction step(s) to which it corresponds. The simple mechanism is a series of sequential thermal losses of CO ligands from increasingly smaller fragments, plus the reverse possible recombination reactions, and the final metal atom or small fragment nucleation process. If the activation energy for the first bond scission is ~4 kcal/mol or more greater than those of the subsequent prenucleation bond scissions, the remaining bonds will be thermally dissociated after the first scission and before the gas cools by thermal conductivity. Recombination will be unimportant and the first bond scission will be rate determining. Experiments were performed to determine if recombination reactions $M(CO)_x + CO \rightarrow M(CO)_{x+1}$ are important to the decomposition kinetics, that is, while the gas is hot, and to ascertain the rate-determining steps.

If recombination kinetics affect the decomposition mechanism, at least a partial equilibrium between $M(CO)_x$ species is established during the reaction time. Addition of CO, even in levels equaling the low carbonyl concentration, should alter such equilibria and affect the decomposition yield. Addition of 5 torr of CO has no effect on iron, molybdenum, and tungsten carbonyl kinetics. Thus, only the decomposition steps are important. (This result also argues against a mechanism of two kinetically significant steps, since such massive amounts of CO would reverse any moderate first-step decomposition via recombination.)

To confirm that the rate-determining step in these processes is indeed the dissociation of the first CO from the complex, trapping experiments were done by adding a large excess of PF_3 to the gas mixture in the cell (~3 torr). Yardley and co-workers[14] have shown that PF_3 can be used as a trapping agent to determine the initial distribution of photofragments resulting from laser photolysis of both $Fe(CO)_5$ and $Cr(CO)_6$. The bond strengths of CO and PF_3 to the transition metals are comparable, and addition of PF_3 to the fragment results in an easily observable complex. If, in fact, the first CO is the strongest bond and all the others are rapidly removed following its dissociation, no products resulting from PF_3 addition to an $M(CO)_{n-x}$ fragment would be seen. On the other hand, if dissociation of the first CO is not the slowest step, all of the $M(CO)_n$ molecules should be

(21) Benson, S. W. "Thermochemical Kinetics", 2nd ed.; Wiley: New York, 1976.

(22) Frurip, D. J.; Bauer, S. H. *J. Phys. Chem.* **1977**, *81*, 1001–1015.

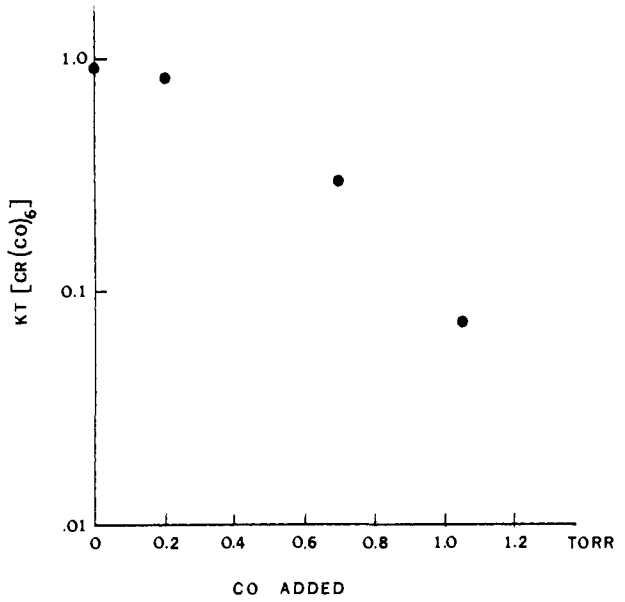

Figure 6. Rate of chromium hexacarbonyl decomposition as a function of CO partial pressure in a 100-torr mixture at a fixed reaction temperature.

rapidly converted to the $M(CO)_{n-x}$ species for which the CO loss *is* the slowest step (i.e., the strongest CO bond). Since only a fraction of this intermediate will then disappear, at a rate dependent upon temperature and reaction time, it should be easily be trapped by the PF_3 once the gas cools.

When either $Fe(CO)_5$, $Mo(CO)_6$, or $W(CO)_6$ was irradiated in the presence of an excess of PF_3, there was no evidence of any trapped products. Runs were done over a range of laser fluences to ensure against the possibility that trapped products were being decomposed in a later laser shot. Therefore, as suggested by the data for added CO, once the first bond breaks these carbonyls are effectively decomposed. No intermediates survive, and the kinetics reflect the initial bond scission reaction step.

The situation for $Cr(CO)_6$ is more complex. Decomposition rates vary with added CO, suggesting a more involved mechanism. Figure 6 shows this variation and indicates that recombination reactions and equilibria occur during the ~ 10 μs of highest temperature reaction time for CO pressures above 0.2 torr. The $Cr(CO)_6$ pressure in the cell was ~ 0.025 torr (0.2-torr vapor pressure[23] at 300 K diluted by 7.6), so even with substantial ligand dissociation, the experrmental CO concentrations are below 0.16 torr at full decomposition. (Other carbonyl concentrations were less.) Thus the rates of Figures 2–5 correspond to the limit of low CO, where recombination reactions play no role in the kinetics of $Cr(CO)_6$ decomposition while the gas is hot. (After the gas is cooled, recombination of undecomposed intermediate fragments with residual CO may still be important.)

When a $Cr(CO)_6$ mixture containing PF_3 is irradiated, mass spectrometric peaks corresponding to $CrPF_3^+$ and $CrCOPF_3^+$ appear. While limits of mass range ($m/e \leq 300$) sensitivity preclude determining exactly the $Cr(CO)_n$ species being trapped, no species were observed with more than one PF_3 ligand attached. This suggests that it is the $Cr(CO)_5$ fragment which is being trapped, since the mass spectrum of $Cr(CO)_4(PF_3)_2$ would have a peak at $Cr(PF_3)_2^+$ and this peak is not observed. In any case, this is a clear indication that $Cr(CO)_6$ thermally decomposes by a different mechanism than that of the other metal carbonyls studied. That is, the first CO to be thermally dissociated from $Cr(CO)_6$ is not the strongest bond but rather a CO dissociated from one of the resulting fragments, probably $Cr(CO)_5$.

Furthermore, when comparative rate measurements were made of the decomposition of $Cr(CO)_6$ relative to dicyclopentadiene

(23) Boxhoorn, G.; Ernsting, J. M.; Stufkens, D. J.; Oskam, A.; *Thermochim. Acta* **1980**, *42*, 315.
(24) Troe, J. *J. Phys. Chem.* **1979**, *83*, 114; **1977**, *66*, 4758.

Table III. $Cr(CO)_6$ First Bond Dissociation

$Mo(CO)_6$, kt_r	T, K	$Cr(CO)_6$, k_1t_r	E_1, kcal/mol (log A = 15.4)
0.048	719	0.321	35.8
0.115	743	1.124	35.2
0.123	745	1.349	35.0
0.066	727	0.568	35.4

in excess PF_3, a large increase in the fractional decomposition of $Cr(CO)_6$ was observed. This rate "enhancement" was such that dicyclopentadiene cannot be considered a suitable standard to use to measure the $Cr(CO)_6$ decomposition rate. This behavior is consistent with a mechanism wherein the first CO bond is relatively weak, resulting in nearly complete conversion from $Cr(CO)_6$ to the $Cr(CO)_n$ species (where $n = 5$ or less), the decomposition of which is the rate-determining step. These molecules, once dissociated, would then lose their remaining CO ligands rapidly, while the $Cr(CO)_n$ molecules which did not react would eventually be cooled, and at the lower temperatures recombine with the small amounts of CO present to re-form $Cr(CO)_6$. Recombination is not thermodynamically favored at the higher reaction temperatures. The process would then be repeated at the next laser shot. Our experiments measure the resulting "steady-state" concentration of $Cr(CO)_6$, i.e., the amount of $Cr(CO)_6$ which remained *after* the recombination step, in essence, a measure of the undecomposed $Cr(CO)_n$. With excess PF_3 present, the change of recombination with a CO was greatly reduced, all undecomposed $Cr(CO)_5$ recombined with PF_3, and we observed the complete dissappearance of the $Cr(CO)_6$ species.

Because of the rapid rate of the first $Cr(CO)_6$ bond scission and the unavailability of a suitable temperature standard faster than dicyclopentadiene, a relative rate plot similar to Figure 2 could not be obtained for $Cr(CO)_6$ with PF_3 trap present. Only a few points at low $Mo(CO)_6$ rate, the fastest carbonyl, and high $Cr(CO)_6$ rate could be measured. Thus, a determination of the activation energy for the first bond dissociation in $Cr(CO)_6$ requires an assumption concerning log A. A reasonable choice is 15.4, both by comparison to the values for other carbonyls determined in this study and to the values typically found for bond scissions producing a diatomic fragment in well-studied organic systems.[21] The results are given in Table III and give an average value of 35.3 ± 0.3 kcal/mol for the $Cr(CO)_6$ first bond dissociation activation energy. An error of 0.5 in the assumed log A corresponds to a 1.7 kcal/mol uncertainty in E_a. With these values for the first $Cr(CO)_6$ decomposition step, the data of Figure 2 can be analyzed to verify the reasonability of our mechanism and to derive an activation energy for the subsequent rate-determining bond cleavage. We assume a two-step mechanism:

$$Cr(CO)_6 \rightleftarrows Cr(CO)_5 + CO \qquad (1, -1)$$

$$Cr(CO)_5 \rightleftarrows Cr(CO)_4 + CO \qquad (2, -2)$$

(The second step in this process, which we are taking as the rate-determining step, could actually be the dissociation of a later fragment if more than one CO is rapidly lost from the parent molecule.) From our experiments we know that (*a*) k_1 is much faster than k_2, (b) k_{-1} and k_{-2}, the recombination reactions, are negligible at high temperature in the low CO limit, and (c) k_2 is rate determining. This leads to the following rate expressions:

$$d[Cr(CO)_6]/dt = -k_1[Cr(CO)_6]$$

$$d[Cr(CO)_5]/dt = k_1[Cr(CO)_6] - k_2[Cr(CO)_5]$$

At low reaction temperatures, the amount of dissociation of the carbonyl fragment in the rate-determining step is small; thus, $k_2[Cr(CO)_5]$ is small relative to $k_1[Cr(CO)_6]$. Therefore,

$$d[Cr(CO)_5]/dt = k_1[Cr(CO)_6]$$

and

$$[Cr(CO)_5]_t = [Cr(CO)_6]_{t=0}(1 - e^{-k_1t})$$

The yield for $Cr(CO)_6$ decomposition for the low-temperature data of Figure 2 is given by

$$k't_r = \int k_2[Cr(CO)_5]dt \cong k_2[Cr(CO)_6]\int_0^{t_r}(1 - e^{-k_1t})dt$$

$$k't_r = k_2t_r[Cr(CO)_6](1 - (1 - e^{-k_1t_r})/k_1t_r)$$

The dicyclopentadiene yield of 0.01 for the lowest temperature point in Figure 2 corresponds to a 740 K temperature. The least-squares line indicates $k't_r = 0.05$, and at this temperature $k_1t_r = 1.10$. This gives a correction factor from the above equation for incomplete $Cr(CO)_6$ initial bond cleavage of 0.394. The derived value of k_2t_r at 740 K is 0.127.

The highest temperature in Figure 2, as revealed by the dicyclopentadiene yield, is 820 K. Here, $k_1t_r = 11.3$, and 90% of the $Cr(CO)_6$ has decomposed to $Cr(CO)_5$ within the first 2 μs of the 10-μs reaction time. Thus, $k't_r$ accurately reflects k_2t_r and has a value of 1.1 at 820 K, by the least-squares line. Again, assuming log A for k_2 of 15.4, these two points give $E_2 = 38.5$ and 39.1 kcal/mol, respectively. Since $E_2 > E_1$, eq 2 is largely the rate-determining step.

Using these two points to derive both Arrhenius parameters results in a low A-factor (log $k_2 = 13.7 - 33/(2.3RT)$). This suggests the correction factor above for $k't_r$ at 740 K is too large and that k_1t may be larger than measured as a result of incomplete trapping. Using only the data of Figure 2, assuming log $A = 15.4$, we obtain $E_2 = 39.1$ kcal/mol and $E_1 = 34.3$ kcal/mol (the 740 K correction factor is 0.59). This is only 1 kcal lower than the E_1 value deduced from the direct trapping experiment.

In addition to the results of Table III and Figure 2, a third experiment is available to determine the $Cr(CO)_6$ first BDE. Assume the data for the CO addition experiment of Figure 6 reflect, roughly, the results of establishing an equilibrium between $Cr(CO)_5$ and $Cr(CO)_6$ shortly after the initial laser heating. The decomposition rate has been halved at 0.5 torr of added CO (1.3 torr at 800 K), meaning $[Cr(CO)_5]/[Cr(CO)_6] = 1.0$. Thus, $K(800\ K) = [CO] = 0.00175$ atm, and given a value of ΔS, we can derive ΔH for dissociation. Approximating the structure of $Cr(CO)_5$ by that of $Fe(CO)_5$ and using known molecular parameters,[14,25,26] we calculate $\Delta S_{800} = 38$ eu. Then $\Delta H°_{800} = 35.6$ kcal/mol ($\Delta H°_{298} = 36.6$ kcal/mol), in close agreement with the kinetically determined values.

The kinetic parameters of interest are those for unimolecular bond scission at high pressure, where the energy-transfer collisions that maintain the tail of the Boltzmann distribution are no longer even partially rate determining. To correct for minor falloff from the high-pressure limit, RRKM-type calculations were performed by using an approach developed by Troe.[24] The required parameters are the bond energy and high-pressure rate constant from these measurements, the carbonyl vibrational frequencies[14,25] and moments of inertia,[26] an average 0.55 kcal/mol energy transferred per collision with N_2,[27] and a 6.4-Å collision diameter.[26,27] A rotational energy correction was calculated for a transition state with a M–C separation given by[21] $r^+/r_0 = (6E_0/RT)^{1/6}$. The results of these calculations are given in Table I and indicate the experimental values are over 80% to the high-pressure limit. The variation in falloff produces small changes in the Arrhenius parameters, typically 0.4 log unit in A and 1 kcal in the activation energy.

Finally, the bond dissociation energy, $\Delta H°_{298}$, must be derived from the activation energy for bond scission at ~750 K. For a loose, hindered rotational transition state with no barrier to recombination at 0 K,[28] $\Delta H°_{298} = E_a - \overline{\Delta C_p°}\ (T - 298) + RT/2$. This correction gives the final values in Table I, with errors estimated to be ~3 kcal/mol.

(25) Shimanouchi, T. *J. Phys. Chem. Ref. Data Suppl.* **1973**, *2*, 121.
(26) Cotton, F. A.; Wilkinson, G. "Advanced Inorganic Chemistry", 4th ed., Wiley: New York, 1980; p 1051.
(27) Barker, J. R. *J. Phys. Chem.* **1984**, *88*, 11.
(28) McMillen, D. F.; Golden, D. M. *Annu. Rev. Phys. Chem.* **1982**, *33*, 493.

Table IV. Metal Carbonyl Bond Dissociation Energies, kcal/mol

compd	$\Delta H°_{298}$ (1)	E (ref 4)	source
$Cr(CO)_6$	36.8	26	this work
$Mo(CO)_6$	40.5	36	this work
$W(CO)_6$	46.0	43	this work
$Fe(CO)_5$	41.5	28	this work
	55 ± 12		ref 31
$Ni(CO)_4$	25 ± 2	35	ref 34
	22		ref 35

Discussion

An initial question is whether these kinetic bond dissociation energies also represent thermodynamic values or whether there is a barrier to recombination, that is, an electronic or steric reorganization energy. The situation is straightforward for $Cr(CO)_6$ and, by analogy, for the other group 6 carbonyls. Matrix spectra[11] indicate a square-pyramidal ground-state structure, and this is corroborated by calculations.[9,10] The lowest state of this symmetry is a $b_2^2e^4$ singlet that correlates with the t_{1g}^6 singlet $Cr(CO)_6$ ground state.[8] Theory indicates no added barrier to dissociation[10] and shows a relatively shallow surface with respect to the equatorial bending motion of the CO ligands.[11] This suggests little barrier to proper rearrangement in the loose transition state and even that the $Cr(CO)_5$ may be very close to its original square-planar configuration in $Cr(CO)_6$. Thus, for group 6, $E_a = \Delta H$.

The d^8 $Fe(CO)_5$ species, however, correlates to a tetrahedral e^4t^4 $Fe(CO)_4$ configuration which has a triplet ground state and will Jahn–Teller distort to C_{3v} or C_{2v} symmetry.[8,11,14] Matrix experiments[11] indicate a high-spin C_{2v} ground state for $Fe(CO)_4$. As a first transition series metal, Fe atomic spectroscopy still significantly reflects electron spin selection rules. Since $Fe(CO)_5$ has the same A-factor as the group 6 carbonyls, its dissociation presumably is the spin-allowed one going to the excited singlet state. The singlet's predicted square planar geometry requires the motion of the two other equatorial CO ligands 30° during dissociation, a minor rearrangement. Thus, the $Fe(CO)_5$ bond dissociation energy determined here likely pertains to dissociations to a singlet product and to ΔH_f (singlet $Fe(CO)_4$).

The remaining discussion includes comparisons of these results with other measurements, an extension by thermodynamic cycles to other ligands, and a brief consideration of photolysis results in light of the bond dissociation energies.

A. Other Measurements. The A-factor of $10^{15.8}$ for $Fe(CO)_5$, and similar values for the other carbonyls, can be compared with reasonable expectations of transition-state theory.[21] This corresponds to $\Delta S^‡ = 10.0$ eu. Consider a simple transition state[29] of reaction path degeneracy 3, with $r^+_{Fe-C}/r_0 = (6E_0/RT)^{1/6}$, a 450-$cm^{-1}$ Fe–C stretch which becomes the reaction coordinate, and two 550-cm^{-1} Fe–C–O bends which become hindered CO rotors in the transition state. With $I^+/I = 1.8$, a completely free CO rotor gives $\Delta S^‡ = 10.2$ eu. If the more typical complete Gorin transition state[29] is used, two 100-cm^{-1} C–Fe–C bends become $Fe(CO)_4$ rotors in the transition state. Then $\Delta S^‡ = 17.7$ eu and the maximum log A is 17.4. If all four transition-state rotors are hindered equally, the observed A-factor corresponds to 84% hindrance, which is a reasonable value compared to previous work with this model.[29] (Note also that log A for NO dissociation from organic systems ranges[21] from 15.6 to 16.3)

The measured carbonyl bond dissociation energies are compared in Table IV to the average bond energy, which is easily derived from gas-phase heat of formation values.[4] It is obvious that the successively cleaved bonds are not of equal strength and that the average value cannot be substituted for the kinetically and thermodynamically correct first bond energy, particularly for the first transition series. This practice has been common in the past, largely because of the lack of reliable values such as those of this study. While emphasizing this caution, however, it should be made clear that such calorimetric measurements can furnish relative bond dissociation energies and provide a basis for estimating

(29) Smith, G. P.; Golden, D. M. *Int. J. Chem. Kinet.* **1978**, *10*, 489.

thermodynamic properties of other compounds by bond enthalpy contributions[4] or group additivity relations in the organic parlance. Secondly, we note our first row transition-metal bond energies are considerably above the low average values, indicating some of the remaining bonds must be very weak. The later transition series, albeit from a limited data base, seem to give bond energies close to the average values. If this is born out by further work, it may prove possible to use the average values rather than make many, more detailed measurements.

Theoretical calculations of these bond energies are difficult and tend to give high values. The 45.8 kcal/mol value of McKinney and Pensak[30] for $Fe(CO)_5$ (low spin) is reasonably close, but the 59 and 50 kcal/mol results[30,10] for $Cr(CO)_6$ show very large error.

Engelking and Lineberger[31] have measured electron affinities for various iron carbonyl fragments by laser photoelectron spectroscopy and have derived neutral bond energies by using mass spectrometric negative ion appearance potentials.[32] The resulting 55 kcal/mol value (see Table IV) is much higher than this measurement but does have a large uncertainty. Also, it should apply to the lower energy triplet $Fe(CO)_4$ ground state. Their bond dissociation energies for the remaining CO ligands, particularly the second bond energy, are all below 32 kcal/mol, which is consistent with our observations of rapid iron formation following a rate-determining initial bond scission. However, the extremely low second bond energy which they report (<14 kcal/mol) is probably too low in view of the $Fe(CO)_5$ photolysis/PF_3 trapping experiments[14] (which trapped $Fe(CO)_4$) and in view of their high first bond energy compared to our value.

Our initial measurement[33] of the $Fe(CO)_5$ bond dissociation energy by laser pyrolysis utilized an infrared fluorescence signal as the thermometer and gave a value of 48 ± 4 kcal/mol. This high value is due to inherent inaccuracies in this method of temperature measurement. A solution measurement[40] on $Fe(CO)_4P(C_6H_5)_3$ gives a 42.5 kcal value, in agreement with our $Fe(CO)_5$ number, but the *A*-factor is higher.

A similar photodetachment measurement[34] on $Ni(CO)_4$ gives a first bond energy of 25 ± 2 kcal/mol, with considerable variation among the various bond strengths, the third being highest (rate determining). A gas-phase $C^{18}O$ ligand substitution study[35] near 300 K gives a similar bond energy value of 22.1 ± 0.4 kcal/mol. This agrees with solution values,[35] but the value of log A = 14.4 is surprisingly low.

A similar series of ligand substitution kinetics investigations, with dissociative mechanisms, has been reported for the group 6 carbonyls, both in solvents at ~100 °C[36] and by ^{14}CO exchange in the gas phase.[37] These results are in general agreement with one another, but differ from the values measured in this study. The reported activation energies for Cr, Mo, and W carbonyls of 39, 30, and 40 kcal/mol compare to our 37, 40, and 46 kcal/mol values. Our parameters predict significantly lower solution rate constants than observed. We also note that a significant S_N2 mechanism occurs in solution[36] especially for the larger metals and that electron-transfer-initiated radical chain mechanisms have also been observed.[41] In the gas-phase work,[37] heterogeneous processes may also be important. One particular piece of evidence in the previous work which suggests a more complex mechanism is the relative *A*-factors. In solution $\Delta S^{\ddagger}$ values vary widely, from ~0 for Mo to ~20 for Cr, while our gas-phase measurements and transition-state theory suggest values of ~10 eu are appropriate for these simple bond scissions. The low solution Mo values in particular suggest a catalytic mechanism.

Recently, Bernstein et al.[42] published the results of a solution photochemistry study of the group 6 hexacarbonyls in which bond dissociation energies were determined by photoacoustic calorimetry. Their values of 37, 34, and 38 (± 5) kcal/mol for Cr, Mo, and W are only lower limits, however, because of possible nonunity quantum yields and metal–solvent interaction for the pentacarbonyl products. Comparison to our results suggests lower quantum yields for $Mo(CO)_6$ and $W(CO)_6$ photodissociation.

B. Derived BDE Values. Having determined the bond dissociation energy for the removal of the first CO ligand from the metal carbonyl, we can now calculate the heat of formation of the $M(CO)_n$ fragment from standard thermodynamic relationships. For example,

$$\Delta H_f[Mo(CO)_5]_g = D[Mo(CO)_5\text{–}CO] + \Delta H_f[CO]_g - \Delta H_f[Mo(CO)_6]_g$$

The gas-phase heats of formation for a variety of monosubstituted metal carbonyl derivatives, $M(CO)_nL$, have been determined from calorimetry and vapor-pressure data. We can, therefore, combine these reported values and the known $\Delta H_f[L]_g$ values with $\Delta H_f[M(CO)_n]_g$ from our experiments to evaluate $D[M(CO)_n\text{–}L]_g$:

$$D[M(CO)_n\text{–}L]_g = \Delta H_f[M(CO)_n]_g + \Delta Hf[L] - \Delta H_f[M(CO)_nL]_g$$

The BDEs for several types of carbonyl derivatives have been calculated in this manner and are reported in Table V.

The amine values require closer examination. The pyridine number for Mo, relative to the carbonyl, appears to be several kilocalories too low by comparison to Cr and W. Pyridine bonds are roughly 6 kcal/mol weaker than CO according to these measurements, indicating the weaker back-bonding of this ligand. One would expect similar values for the aromatic pyrazine and pyrazole systems, but the Cr data are particularly scattered and probably unreliable. The W compounds are more easily synthesized, handled, and measured. A further 5 kcal weakening of the metal–nitrogen bond appears to occur for these ligands.

Table V. Derived Bond Energies

$M(CO)_nL$	ΔH_f-$[M(CO)_nL]_g$, kcal/mol	D-$[M(CO)_n - L]_g$, kcal/mol
$Mo(CO)_5CO_b$	−218.7	40.5
$Mo(CO)_5$–piperidine[a]	−206.7	43.7
$Mo(CO)_5$–pyridine[a]	−147.9	29.7
$W(CO)_5CO$[b]	−211.3	46.0
$W(CO)_5$–piperidine[a]	−194.8	44.7
$W(CO)_5$–pyridine[a]	−144.8	39.5
$W(CO)_5$–pyrazine$_a$	−127.4	35.5
$W(CO)_5$–pyrazole[a]	−126.4	33.0
$W(CO)_5NCCH_3$[c]	−164.0	42.7
$Fe(CO)_4CO$[b]	−173.0	41.5
$Fe(CO)_4C_2H_4$[b]	−129.8	37.2
$Fe(CO)_4Fe(CO)_5$[b]	−319.1	9.8
$Cr(CO)_5CO$[b]	−217.0	(36.8)
$Cr(CO)_5$–piperidine[a]	−199.8	(34.8)
$Cr(CO)_5$–pyridine[a]	−150.3	(30.1)
$Cr(CO)_5$–pyrazine[a]	−127.6	(20.8)
$Cr(CO)_5$–pyrazole[a]	−144.1	(35.8)

[a] Reference 38. [b] Reference 4. [c] Reference 39.

(30) McKinney, R. J.; Pensak, D. A. *Inorg. Chem.* **1979**, *18*, 3413.
(31) Engelking, P. C.; Lineberger, W. C. *J. Am. Chem. Soc.* **1979**, *101*, 5569.
(32) Compton, R. N.; Stockdale, J. A. D. *Int. J. Mass Spectrom. Ion Phys.* **1976**, *22*, 47.
(33) Smith, G. P.; Laine, R. M. *J. Phys. Chem.* **1981**, *85*, 1620.
(34) Stevens, A. E. *Feigerle*, C. S.; Lineberger, W. C. *J. Am. Chem. Soc.* **1982**, *104*, 5026.
(35) Day, J. P.; Basolo, F.; Pearson, R. G. *J. Am. Chem. Soc.* **1968**, *90*, 6927.
(36) Graham, J. R.; Angelici, R. T. *Inorg. Chem.* **1967**, *6*, 2082. Werner, H.; Prinz, R. *Chem. Ber.* **1966**, *99*, 3582.
(37) Pajaro, G.; Calderazzo, F.; Ercoli, R. *Gazz. Chim. Ital.* **1960**, *90*, 1486. Cetini, G.; Gambino, O. *Atti. Accad. Sci. Torino, Cl. Sci. Fis. Mat. Nat.* **1963**, 757, 1197.
(38) Daamen, H.; Van der Poel, H.; Stufkens, D. J.; Oskam, A. *Thermochim. Acta* **1979**, *34*, 69.
(39) Martinho-Simões, J. A. private communication. Bleijerveld, R. H. T.; Vrieze, K. *Inorg. Chem. Acta* **1976**, *19*, 195. Adedeji, F. A. Connor, J. A.; Demain, C. P.; Martinho-Simões, J. A.; Skinner, H. A.; Moattar, M. T. Z. *J. Organomet. Chem.* **1978**, *149*, 333.
(40) Siefert, E. E.; Angelici, R. J. *J. Organomet. Chem.* **1967**, *8*, 374.
(41) Hershberger, J. W.; Klinger, R. J.; Kochi, J. K. *J. Am. Chem. Soc.* **1983**, *105*, 61.
(42) Bernstein, M.; Simon, J. D.; Peters, K. S. *Chem. Phys. Lett.* **1983**, *100*, 241.

The acetonitrile value for tungsten is quite close to the CO bond strength. This seems unlikely, in view of its very labile behavior in solution where it can be replaced by olefins.[43] Finally, the results suggest piperidine is as strongly bound a ligand as CO and stronger than the aromatic pyridine. This may be indicative of its greater strength as a base. Both solution kinetic and photochemistry work,[44] however, indicate piperidine is a more labile ligand than CO toward substitution.

The value given for $Fe_2(CO)_9$ involves breaking three bridging CO bonds. The low number for this stable compound is a thermodynamic, rather than kinetic, one, as might be expected for such a complex dissociation process. The bond energy for the ethylene π electrons to $Fe(CO)_4$ has an expected lower value. This number has mechanistic implications, since $Fe(CO)_5$ photolysis fragments, probably $Fe(CO)_3$, are known to catalyze olefin rearrangement and hydrogenation[13] reactions. Turnover rates will depend on the strengths of iron–ethylene bonds.

C. Photochemistry Comparisons. Many photochemical experiments[11-16] have been undertaken on metal carbonyls in recent years, and the bond energies of this study can be of use in interpreting some of them. Breckenridge and Sinai[12] photolyzed $Cr(CO)_6$ at 355 nm (80 kcal/mol) to produce $Cr(CO)_5$. Our results indicate the use of almost all this energy (77 kcal/mol) would have been necessary to produce singlet $Cr(CO)_4$. Yardley and co-workers,[14] however, photolyzed at 248 nm (115 kcal/mol), in the gas phase, with a PF_3 trap. They observed large yields of $Cr(CO)_4$, a little $Cr(CO)_5$, and some $Cr(CO)_2$ and $Cr(CO)_3$. The difference in the two photolysis studies is readily interpreted in terms of the new bond dissociation energy values but not on the basis of average bond energies. From the 248-nm results, one can also determine that the third and fourth bond energies total less than 38 kcal/mol, while the final two together are greater than 39 kcal/mol. Fletcher and Rosenfeld have observed the time evolution of CO product by laser absorption spectroscopy.[16] They observed both a rapid initial decay channel and two longer time decarbonylation steps. These are assigned to slow sequential dissociations in the triplet manifold, since our bond energy values would predict rapid loss of the first two CO's in the singlet ground state according to RRKM estimates (the fast process).[16] It thus appears that the interpretation of photolysis results for group 6 carbonyls requires energetics information for both electron spin configurations.

Photolysis trapping experiments have also been reported[14] for $Fe(CO)_5$ at 352, 248, and 193 nm. The relatively even yields of $Fe(CO)_n$, n = 2, 3, 4, at the lowest 81 kcal/mol energy suggest that the second bond energy is not as weak as first thought,[31] but our results would imply that the second and third bond energies add up to less than 40 kcal/mol. The alternate explanation for the photolysis results is production of the triplet, ground-state $Fe(CO)_4$, which should take less energy than our measured 41.5 kcal bond energy. Recently, Ouderkirk et al.[15] observed the transient absorption spectra of $Fe(CO)_n$ photolysis fragments, at various added CO pressures. Recombination kinetics for n = 2 or 3 were much faster than for n = 4, which is consistent with a crossing of spin states upon going from n = 5 to 4.

In summary, these photolytic systems provide contrasting behavior when compared to the thermal decompositions examined in this study. The necessity of considering triplet states and the ability to generate only partially decomposed unsaturated species are two such features. Except for $Cr(CO)_6$, the homogeneous thermal decomposition of these metal carbonyls proceeds to completion, resulting in metal particulate products. (This is also true for $Mn_2(CO)_{10}$.) Trapping experiments indicate that the first bond scission is usually rate determining. In addition to providing kinetic results and aiding in the interpretation of other experiments, these thermal measurements provide, for the first time, some much needed thermodynamic data on transition-metal–ligand bond dissociation energies.

The bond dissociation energy results of this study indicate that the first row transition-metal carbonyl values differ greatly from the average energy of all the bonds, while the later, heavier metal carbonyl bond energies are close to the average values. The pyridine ligand is bound more weakly than CO, while the nonaromatic piperidine roughly equals CO in bond energy. More thermodynamic data are needed to derive bond dissociation energies for nonaromatic ligands, and many other metals remain to be kinetically investigated in similar studies.

Acknowledgment. This work was supported by the National Science Foundation under Grant CHE79-23569 and is based on a thesis submitted to the Chemistry Department of San Jose State University in partial fulfillment of requirements for a M.S. degree (K.E.L.). We thank Dr. R. Laine (SRI) for useful discussions and Professor N. Albert (San Jose State University) for his assistance (K.E.L.). We also thank Professor S. W. Benson, Professor J. L. Beauchamp, Dr. J. A. Martinho-Simões, and the referees for their suggestions.

Registry No. $Mo(CO)_6$, 13939-06-5; $Mo(CO)_5$-piperidine, 19456-57-6; $Mo(CO)_5$-pyridine, 14324-76-6; $W(CO)_6$, 14040-11-0; $W(CO)_5$-piperidine, 31082-68-5; $W(CO)_5$-pyridine, 14586-49-3; $W(CO)_5$-pyrazine, 65761-19-5; $W(CO)_5$-pyrazole, 39017-11-3; $W(CO)_5NCCH_3$, 15096-68-1; $Fe(CO)_5$, 13463-40-6; $Fe(CO)_4C_2H_4$, 32799-25-0; $Fe(CO)_4Fe(CO)_5$, 15321-51-4; $Cr(CO)_6$, 13007-92-6; $Cr(CO)_5$-piperidine, 15710-39-1; $Cr(CO)_5$-pyridine, 14740-77-3; $Cr(CO)_5$-pyrazine, 66179-02-0; $Cr(CO)_5$-pyrazole, 71127-65-6.

(43) King, R. B.; Fronzaglia, A. *Inorg. Chem.* **1966**, *5*, 1837.
(44) Covey, W. D.; Brown, T. L. *Inorg. Chem.* **1983**, *12*, 2820. Dennenberg, R. J.; Darensbourg, D. J. *Ibid.* **1972**, *11*, 72. Wrighton, M. *Ibid.* **1974**, *13*, 905. Darensbourg, D. J.; Murphy, M. A. *Ibid.* **1978**, *17*, 884.